Squeeze flow behaviors of magnetorheological plastomers under constant volume

Yangguang Xu (许阳光), Xinglong Gong (龚兴龙),[a] Taixiang Liu (刘太祥), and Shouhu Xuan (宣守虎)

CAS Key Laboratory of Mechanical Behavior and Design of Materials, Department of Modern Mechanics, University of Science and Technology of China (USTC), Hefei 230027, Anhui, China

(Received 6 November 2013; final revision received 12 March 2014; published 26 March 2014)

Synopsis

The squeeze flow behaviors (including compressive, tensile, and oscillatory squeeze behaviors) of magnetorheological plastomers (MRPs, a kind of solidlike magnetic gels) under different experimental conditions are systematically investigated. Both compression and tension processes can be classified as elastic deformation region, stress relaxation region, and plastic flow region. A squeeze flow equation is used to describe the compressive behaviors of MRP in plastic flow region from which the compressive yield stress can be obtained and compared. The results demonstrate that both compressive yield stress and tensile yield stress are sensitive to magnetic field, particle distribution, and particle concentration. The yield stress of MRP under squeeze flow is larger than that of MR fluids due to the existence of polymer matrix. Asymmetry of hysteresis loop is found under oscillatory squeeze mode. The oscillatory squeeze behaviors of MRP are also influenced by magnetic field and particle concentration, but the influence of particle distribution is not so obvious. The related results under three operational modes are compared and qualitatively analyzed, which are helpful for further understanding the MR mechanism in the solidlike magnetic gels. © *2014 The Society of Rheology*. [http://dx.doi.org/10.1122/1.4869350]

I. INTRODUCTION

Magnetorheological (MR) materials are a kind of magneto-sensitive smart materials whose rheological properties can be controlled by an external magnetic field. MR fluids, as one of the important branch of MR materials, have been extensively studied from both physical mechanisms and applications. Olabi and Grunwald (2007) classified MR fluids operation into direct shear mode, valve mode, and squeeze flow mode depending on the flow mode and the rheological stress of MR fluids. Most MR fluids based devices are designed working under these three operational modes or their combination. In comparison with the other two operational modes, the devices based on squeeze flow mode are rarely reported though the yield stress of MR fluids under this mode would be up to one order of magnitude larger than that under direct shear mode or valve mode. The

[a]Author to whom correspondence should be addressed. Fax: +86 551 63600419. Electronic address: gongxl@ustc.edu.cn

magneto-induced particle aggregates and the magnetic interaction between them are believed to be the key reasons for the MR effect [de Vicente *et al.* (2011b)]. The flow mode will affect the formation of magneto-induced microstructure and further affect the MR performance. Therefore, more and more researchers focused their interests on the rheological properties of MR fluids under squeeze flow mode and related MR mechanisms for its potential application prospect in recent years.

As an analogy of field-responsive smart materials, the squeeze flow behaviors of electrorheological (ER) fluids were first and thoroughly investigated [Choi *et al.* (2005); Chu *et al.* (2000); McIntyre and Filisko (2007); See *et al.* (1999); Tian and Zou (2003); Yang (1997)]. The characterization technologies and the squeeze mechanisms of ER fluids can be used for references to the investigation on the squeeze flow behaviors of MR fluids. Tang *et al.* (2000) found a compressive load along the magnetic field will greatly increase the static yield stress of MR fluids for the squeeze-strengthen effect induced by compression. Zhang *et al.* (2004) further studied this squeeze-strengthen effect experimentally. At the same time, a theoretical approach was employed to explain the experimental results. The compressive stress-strain curves of MR fluids under different magnetic fields, initial gaps, and compressive speeds were obtained by Mazlan *et al.* (2007). They divided the compression curves into three regions and discussed the dependence of the curve shape on the different squeeze conditions [Mazlan *et al.* (2008a)]. The aforementioned results were tested under constant area compression. The concentration of particles and the volume of the sample between the parallel plates changed because the fluidic matrix was squeezed out during the compression and the magnetic particles would aggregate between parallel plates under magnetic field. This was named as "sealing effect" and would affect accurate understanding of squeezing mechanism. McIntyre and Filisko (2007) pointed out that the constant volume compression could avoid this problem. de Vicente *et al.* (2011a) investigated the squeeze flow behaviors of MR fluids under constant volume operation. Different squeeze flow models and particle-level dynamic simulation were compared with the experimental results. Both theoretical and experimental approaches verified that the squeeze-strengthen effect was relevant with the structure reorganization. Further, they studied the influence of magnetic field, medium viscosity, and particle concentration on the performance of MR fluids under constant volume compression mode [Ruiz-Lopez *et al.* (2012)]. A similar experimental research was also presented by Guo *et al.* (2013).

The tensile behavior is another important aspect to comprehend the structural evolution mechanism of MR fluids compared to the compressive behavior. Unfortunately, little attention has been paid to the tensile behavior of MR fluids except for the works reported by Mazlan *et al.* (2011), Mazlan *et al.* (2008b), Wang *et al.* (2011), and Wang *et al.* (2013). The experimental results demonstrated that there was a difference between tensile behavior and compressive behavior, which indicated that different structural evolution mechanisms might exist in the two kinds of squeezing modes. In addition, there seems no report about the investigation on the oscillatory squeeze behavior of MR fluids. Some preliminary applications by using MR fluids working under squeeze mode in damper [Ahn *et al.* (2004); Carmignani *et al.* (2006); Kulkarni *et al.* (2003); Wang *et al.* (2005)] and mount [Farjoud *et al.* (2011)] have been tried; superior performance was presented in these squeeze-film dampers than that of the devices working under shear mode.

However, the intrinsic sedimentation problem and leakage in the application devices of conventional MR fluids become the bottlenecks for their wide application [de Vicente *et al.* (2011b); Park *et al.* (2010)]. Therefore, except for further improving these drawbacks, a lot of works have been done to seek the substitutes of MR fluids [Chen *et al.* (2007); Fuhrer *et al.* (2009); Li *et al.* (2010); Mitsumata and Abe (2009); Nguyen *et al.*

(2012); Wilson *et al*. (2002)]. Among them, a novel kind of solidlike magnetic gels was developed recently [An *et al*. (2010); Mitsumata and Ohori (2011); Xu *et al*. (2011)]. No particle sedimentation exists in these solidlike magnetic gels; the particles will rearrange to form chainlike or columnlike structures along the direction of magnetic field, and the microstructure can be retained after removing the magnetic field. These merits make the solidlike magnetic gels a promising candidate to substitute conventional MR fluids in some applications. Previous researches indicated that the solidlike magnetic gels show some interesting properties different from MR fluids due to the existence of polymer matrix [An *et al*. (2012); Mitsumata *et al*. (2012); Xu *et al*. (2012)]. Nevertheless, the understanding on the MR mechanism of the solidlike magnetic gels is not deep enough, while the characterization on the mechanical properties of them is not comprehensive as well. As an important characterization method we have mentioned above, the rheological properties of the solidlike magnetic gels under squeeze flow mode are very important for further understanding the MR mechanism, which have not been assessed before, unfortunately.

In this work, the squeeze flow behaviors (including compressive, tensile, and oscillatory squeeze behaviors) of MR plastomers (MRPs, a kind of solidlike magnetic gels) [Xu *et al*. (2011)] were experimentally studied. The influences of magnetic field strength, particle distribution, and particle concentration on the three squeeze methods were compared, respectively. The main concerns are the unique squeezing behaviors of MRP and the differences on the rheological properties under different squeezing modes. At the same time, the squeezing mechanisms of MRP were discussed under different squeezing modes based on the experimental results.

II. EXPERIMENTAL

A. Materials

The MRP is a kind of solidlike magnetic gels prepared by mixing micrometer sized carbonyl iron particles (Type CN, provided by BASF in Germany with an average radius of 6 μm) with a plastic polyurethane matrix. The detail of synthetic process of polyurethane matrix is from our previous work [Gong *et al*. (2012)]. In this work, five different MRP samples with different weight fractions were prepared. We name these MRP samples as MRP-40, MRP-50, MRP-60, MRP-70, and MRP-80 corresponding to 40%, 50%, 60%, 70%, and 80% weight fraction of iron particles, respectively (corresponding to 8.4%, 12.1%, 17.0%, 24.2%, and 35.4% in volume fraction, respectively). All the sample were preprocessed under a 667 mT magnetic field (the coil current density is 1.25 A when the gap between parallel plates is 2 mm) for 5 min unless otherwise specified. The preprocessed sample is anisotropic with chainlike or columnlike microstructures, which have been discussed in our previous work [Gong *et al*. (2012); Xu *et al*. (2011)].

B. Apparatus and experimental principle

The squeeze behaviors of MRP were investigated by INSTRON dynamic and static test instrument (Type Electropuls™ E3000, INSTRON Co., USA). The compressive, tensile, and oscillatory squeeze tests can be easily achieved by the instrument. Its dynamic load capacity is ± 3000 N, while the static load capacity is ± 2000 N, which is an ideal testing range for our MRP sample. The displacement excitation controlled by the preset program is applied from the upper grip of INSTRON, and the signal of response force will be collected by the sensor connected to the lower grip. Figure 1(a) shows the picture of measurement system. A pair of cylinders made of pure iron twined by Helmholtz coils

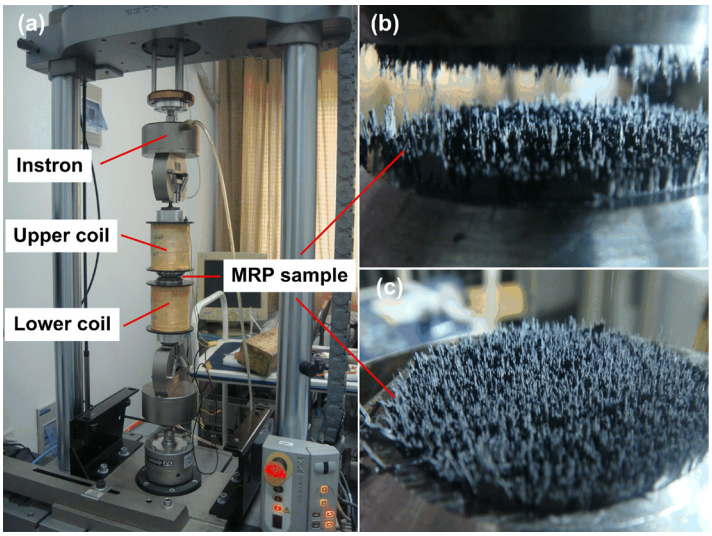

FIG. 1. The measurement system (a) and the MRP sample after a tensile test is completed under an external magnetic field: Axonometrical drawing (b) and the detail of MRP (c).

(3200 turns) is clamped by the upper and lower grips of INSTRON. The Helmholtz coils are connected with two current sources, respectively. The magnetic field is generated by the Helmholtz coils, and the magnetic field strength can be controlled by adjusting the current density through the coils. The iron cylinders will enhance the magnetic field strength except as the parallel plates contacting with the MRP samples. The contact zones of cylinders with sample are processed smoothly with diameters of 50 mm and parallel to each other.

The magnetic flux density between parallel plates was measured by a tesla meter (type HT 20, the resolution is 1 mT in the measuring range of 0–2000 mT, Shanghai Hengtong magnetic technology Co., Ltd, China), as shown in Fig. 2. At a fixed gap size between parallel plates, the magnetic flux density will increase with the increase of current density. Another valuable conclusion is that the magnetic flux density will decrease with the increase of plate gap for different current densities, and an inverse relationship can be found between them. We fit the experimental results with linear functions so the magnetic flux density at any gap between 1 and 2 mm can be obtained. Moreover, the magnetic flux densities at every position between the parallel plates (the result is not shown here) were measured. It was found that the magnetic field distribution is uniform, which is coincident with the results obtained by Guo *et al*. (2013).

The experimental approach to obtain the compressive (or tensile) force F of MRP under various conditions is explained in detail in the supplementary information. After F is obtained, we define the average normal stress as

$$\sigma = \frac{F}{S} = \frac{F(h_0 - h_t)}{V}. \tag{1}$$

The contact area S ($S = \pi r^2$, r is the radius of MRP) is calculated by the ratio of constant volume of MRP sample V to the current gap size h. The current gap size h is the difference between the initial gap h_0 and the distance h_t that the upper plate moves during the compression (i.e., $h = h_0 - h_t$). If the upper plate moves along the opposite direction (i.e., tensile test), h is the sum of h_0 and h_t. V was set as 1.964 ml, which will make the MRP

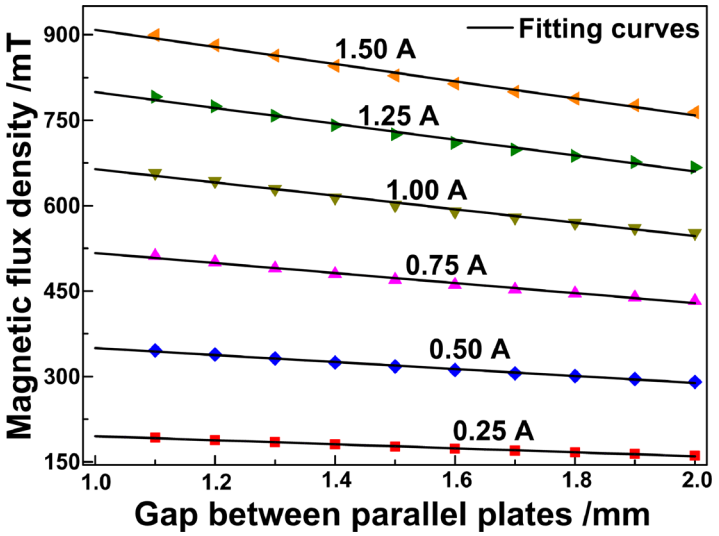

FIG. 2. Magnetic flux densities between parallel plates at different current densities and gap sizes. The solid lines are linear fitting curves for different current densities.

overspread the whole surface of the plates when the gap size reduces to 1 mm. The squeeze strain is expressed as

$$\varepsilon = \frac{h_t}{h_0}. \tag{2}$$

Besides, all the tests were conducted at room temperature.

III. RESULTS AND DISCUSSION

A. Compressive behaviors of MRP

Figure 3 demonstrates the magneto-induced normal stress of MRP under different magnetic fields, which is measured by a parallel-plate rheometer (Physica MCR 301, Anton Paar Co., Austria). The measurement approach is the same as the one presented by Liu *et al.* (2013a) The normal stress originates from the magnetostriction effect of MRP. When a magnetic field is applied to MRP, a trend of extension along with the magnetic field direction generates. However, the MRP is confined by the parallel plates. A squeezing force to the plates corresponding to the normal stress will then be induced. The normal stress increases with the increase of magnetic flux density and particle concentration, indicating the magnetostriction effect will be enhanced by an external magnetic field and particle concentration. A particle-level dynamic simulation demonstrated that the magnetic interaction force between the particles which is sensitive to the applied magnetic field is closely related to the magneto-induced normal stress of MRP [Liu *et al.* (2013a)]. On the other hand, the magnetic interaction force between the particles can also be calculated by integrating the Maxwell stress over a closed contour around one of the particles [Gomez-Ramirez *et al.* (2011)]. In other words, Maxwell stress can be regarded as the source of magneto-induced normal stress of MRP. Normal stress is an important magneto-induced rheological property of MRP but is unrelated to the squeeze flow behaviors of MRP. Therefore, it should be excluded from the resultant force when considering the squeeze flow behaviors of MRP (the details can be found in the supplementary information).

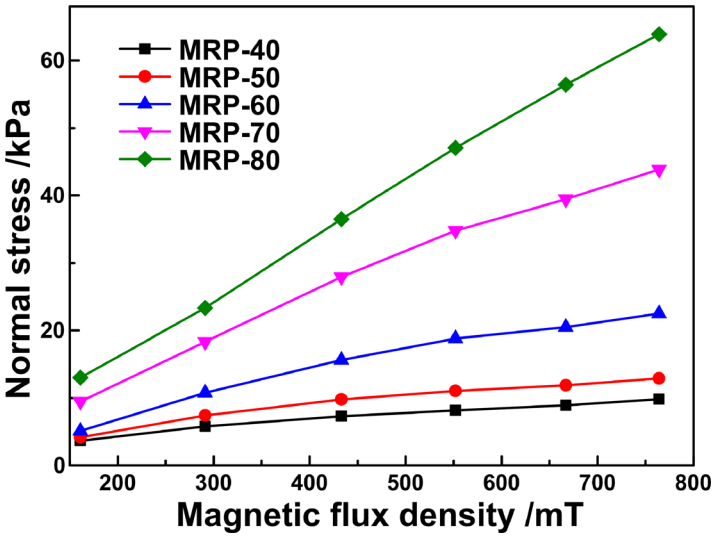

FIG. 3. Normal stress of MRP with different particle concentrations under different magnetic fields.

The squeeze flow theories of inelastic yield fluids have been completely reviewed by de Vicente *et al*. (2011a) They analyzed the squeezing behaviors of MR fluids under constant volume based on the squeeze flow equation

$$F = \frac{2\tau_y V^{3/2}}{3\sqrt{\pi}h^{5/2}}, \tag{3}$$

where τ_y is the shear yield stress of MR fluid, V and h have the same meanings as given in Sec. II. No-slip hypothesis and low plasticity number ($S_P \ll 1$) condition are established if the squeeze flow equation is reasonable to describe squeezing behaviors of MR fluids. The plasticity number S_P is defined as follows:

$$S_P = \frac{\eta_P \nu r}{h^2 \tau_y}, \tag{4}$$

where η_p and v represent the Bingham plastic viscosity and the compressive speed, respectively. Here, we will discuss the validity of adapting the squeeze flow equation to the case of MRP. As shown in Figs. 1(b) and 1(c), the MRP sample will firmly stick to the plates even if fractured near the middle when subjected to a tensile load. Therefore, it is believed that the no-slip hypothesis is reasonable corresponding to the compressive behaviors of MRP. As for another condition, S_P will be conservatively estimated as follows based on our previous work [Xu *et al*. (2013)]:

$$S_P = \frac{\eta_P \nu r}{h^2 \tau_y} < 3.4 \times 10^{-3} \ll 1, \tag{5}$$

which means that yield shear stress plays a leading role in the compression deformation of MRP. Next, the possible influential factors including magnetic field, compressive speed, initial compressive gap, particle distribution, and particle concentration to the compressive force of MRP will be discussed, respectively.

The attractive force of parallel plates increases with the increasing magnetic field and compressive strain, as shown in Fig. 4(a). It is worth noting that the magnetic field

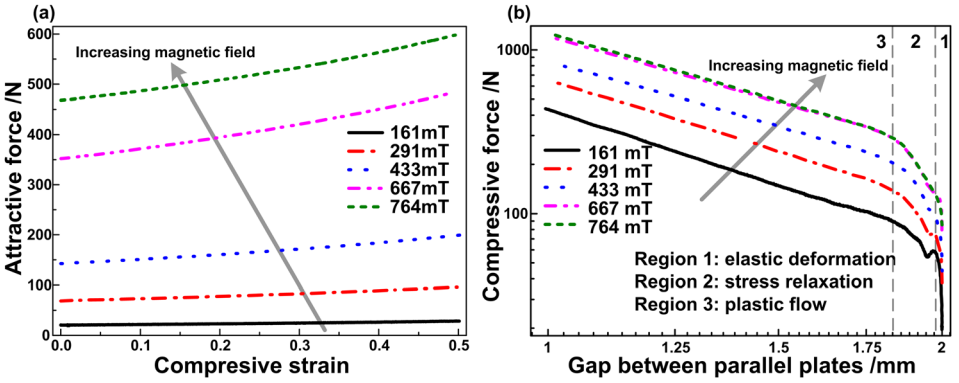

FIG. 4. (a) Attractive forces of parallel plates under different compressive strains and magnetic flux densities. (b) Compressive force of MRP-70 vs gap between parallel plates under different magnetic fields in double logarithmic presentation. The initial gap between parallel plates is 2 mm and the compressive velocity is 0.5 mm/min. The magnetic flux density after the legend represents the value at the initial gap size.

strength will change with the increase of strain (Fig. 2) and the value after the legend is the initial magnetic flux density when the compressive strain is zero (i.e., the gap between parallel plates is 2 mm). Unlike MR fluids, three regions can be observed from the compressive curves of MRP in double logarithmic presentation. As shown in Fig. 4(b), an obvious stress relaxation region (region 2) can be found between elastic deformation region (region 1) and plastic flow region (region 3). The elastic deformation region and plastic flow region also exist in MR fluids [Guo *et al*. (2013)]. The interval of region 1 is narrow (1.98–2 mm), so the particle chains have not ruptured obviously by the compressive strain in this region. The elastic deformation of particle chains and polymer matrix is the dominating deformation mechanism in this region. In the elastic deformation region, the gap between adjacent particles will decrease and the polymer matrix filled in the particle chains will be squeezed out. Therefore, the particle chains will become more compact due to the compression of upper plate. The compact chainlike structures will enhance the resistance of MRP to deformation, which is the so-called squeezing-strengthen effect [Tang *et al*. (2000); Zhang *et al*. (2004)]. With the further decreasing of gap size, the structure failure of particle chains and the relaxation phenomenon originating from polymer matrix can be observed clearly. Both destruction of particle chains (here means bending instability of particle chains under compression) [Liu *et al*. (2013b)] and relaxation of polymer matrix will affect the resistance of MRP to deformation. As a result, compressive force increases slowly in region 2 compared with the elastic deformation region. This is a unique region for MRP due to the existence of polymer matrix. A linear relationship between compressive force and gap size in log-log coordinate can be found in region 3. It is believed that the squeeze flow equation can be employed to describe the plastic flow behavior of inelastic materials. However, deviations from theoretical model in experimental results which cannot be neglected were found in MR fluids [Ruiz-Lopez *et al*. (2012)]. These deviations may ascribe to the changes of experimental conditions and materials properties. For further analyzing the squeeze flow behaviors of MRP, we rewrite the relationship of compressive force and gap size as

$$F = kh^n, \tag{6}$$

where k is a constant parameter related to the material characteristics of MRP and n is the slope of F and h in the log-log coordinate. Actually, Eq. (6) is the general form of

squeeze flow equation. Based on the squeezing flow equation, we can fit the curves under different experimental conditions in region 3 and analyze the reason for the deviation of related parameters in experiment from theory. What is more, the compressive yield stress σ_C can be calculated according to Eq. (1) at the position of demarcation point of regions 2 and 3.

Magnetic field will change the compressive resistance of MRP to deformation by controlling the magnetic interactions between particles. Therefore, the compressive force increases with the increase of magnetic field at a fixed gap size [Fig. 4(b)]. The fitting parameters k and n in the plastic flow region increase with the increase of magnetic field (as shown in Table I). The increasing k suggests the increase of shear yield stress by comparing Eq. (3) and Eq. (6). It is noticed that the values of n under different magnetic fields are close to the theoretical value ($n = -2.5$), which demonstrates that MRP tends to the ideal inelastic material described by squeeze flow equation under an external magnetic field. At the beginning of plastic flow, the compressive yield stress σ_C increases with the increase of magnetic field as well. σ_C increases 3.23 times when the magnetic flux density changes from 161 to 764 mT, a typical MR effect. This magneto-sensitive compressive property of MRP shows saturation phenomenon (i.e., σ_C almost keep constant when the magnetic flux density exceeds 667 mT), which is relevant with the saturation magnetization of carbonyl iron particles and is also found in shear operational mode [Xu *et al.* (2011)].

The attractive force of parallel plates increases slightly with the increase of compressive speed [Fig. 5(a)]. A similar trend for the compressive force of MRP can be observed from Fig. 5(b), but the influence of compressive speed is more obvious. Interestingly, an opposite relationship between compressive force and speed was found in MR fluids [Guo *et al.* (2013)] and ER fluids [McIntyre and Filisko (2010)]. McIntyre and Filisko (2010) pointed out that for ER fluids with high viscosity matrix, where the "filtration" (i.e., the separation of particles from fluid matrix) will not occur under compression, the viscous force from the matrix will contribute to the resistance to the deformation a lot. At the same time, the contribution of resistance from particle chains under the same magnetic

TABLE I. The fitting parameters of MRP in the plastic flow region under the different conditions.

Particle distribution	W (wt. %)	B (mT)	v (mm/min)	h_0 (mm)	k	n	σ_C (kPa)
Isotropic	70	0	0.5	2.0	284.25	−4.32	19.06
Anisotropic	70	0	0.5	2.0	372.74	−3.87	38.08
Anisotropic	70	161	0.5	2.0	432.12	−2.62	84.10
Anisotropic	70	291	0.5	2.0	659.55	−2.48	130.02
Anisotropic	70	433	0.5	2.0	856.29	−2.34	190.29
Anisotropic	70	667	0.5	2.0	1210.51	−2.27	269.80
Anisotropic	70	764	0.5	2.0	1269.64	−2.27	271.43
Anisotropic	70	433	0.1	2.0	726.42	−2.25	159.59
Anisotropic	70	433	1.0	2.0	992.29	−2.39	217.95
Anisotropic	70	433	1.5	2.0	1148.63	−2.42	251.23
Anisotropic	70	433	2.0	2.0	1198.75	−2.54	230.83
Anisotropic	70	433	0.5	2.5	864.39	−2.32	144.57
Anisotropic	70	433	0.5	3.0	888.73	−2.31	105.01
Anisotropic	40	433	0.5	2.0	225.56	−2.51	51.77
Anisotropic	50	433	0.5	2.0	298.75	−2.46	59.74
Anisotropic	60	433	0.5	2.0	405.29	−2.38	90.21
Anisotropic	80	433	0.5	2.0	1282.33	−2.13	305.42

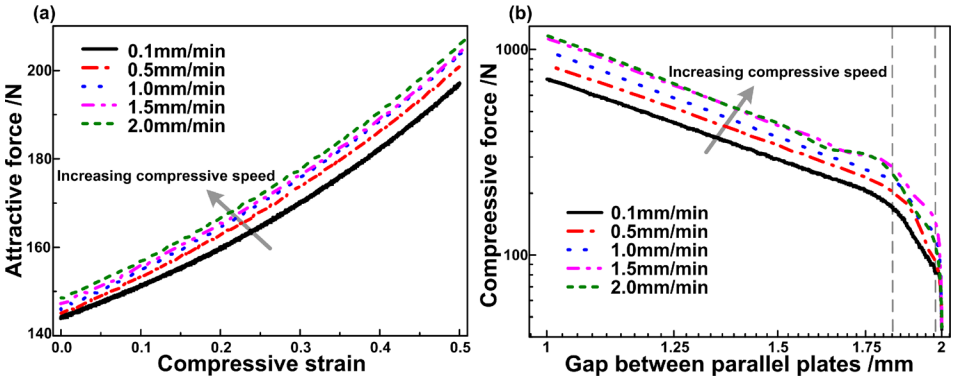

FIG. 5. (a) Attractive forces of parallel plates under different compressive strains and speeds. (b) Compressive force of MRP-70 vs gap between parallel plates at different compressive velocities in double logarithmic presentation. The initial gap between parallel plates is 2 mm and the corresponding magnetic flux density is 433 mT.

field only depends on the gap size. That is to say, the compressive force from the particle chains is independent on the compressive speed. Therefore, the polymer matrix probably plays a key role in the speed-enhanced effect of MRP. High compressive speed will lead to a large repulsive viscous force from polymer matrix, which is contributed to the total compressive force. It is also noticed that k and σ_C increases with the increase of compressive speed (Table I), suggesting that the contribution of polymer matrix to the yield stress is also important compared with the magneto-induced effect. It should also be mentioned that the relaxation of polymer matrix is relevant with time, so the intervals of region 2 vary with the change of compressive speeds. However, we found that the slope of region 3 is not influenced by the relaxation phenomenon and the compressive speed [Fig. 5(b)]. As a result, we still regard the same position as the beginning of plastic flow region (region 3 is dependent on the moving distance of upper plate) and the stress relaxation region is partly overlapping with the plastic flow region under high compressive speed.

The compression tests were carried out at different initial gap sizes to further understand the gap dependence of compressive force of MRP in a wide range. As expected, the attractive force of parallel plates monotonically decreases with the increase of gap size [Fig. 6(a)]. Well overlap of three attraction curves demonstrates the experimental error is negligible. The overlap of compressive curves in region 3 (the fitting parameter n is

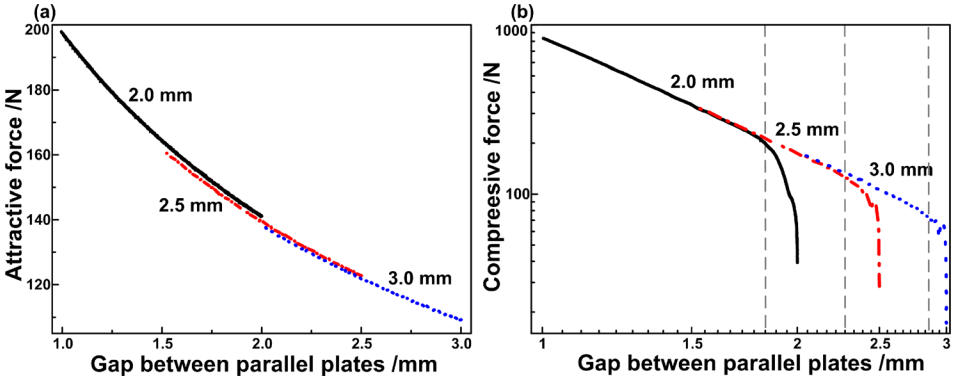

FIG. 6. (a) Attractive forces of parallel plates under different initial gap sizes between parallel plates. (b) Compressive force of MRP-70 vs gap between parallel plates in double logarithmic presentation. The compressive velocity is 0.5 mm/min and the magnetic flux density is 433 mT.

almost the same under different initial gap sizes as shown in Table I) also proves that the plastic flow of MRP is decided by the moving distance of upper plates but not the initial gap size. The same k value under different initial gap sizes suggests that the shear yield stress is also independent on the initial gap size. However, the compressive yield force presents decreased trend with the increase of initial gap size. Ruiz-Lopez *et al.* (2012) discussed the relationship between τ_y and σ_C under squeeze flow. Here, we write an equivalent expression to qualitatively analyze the experimental phenomenon

$$\sigma_C = \frac{2\tau_y V^{3/2}}{3\pi^{3/2}(h_0 - h_c)^{5/2}} = \frac{2\tau_y V^{1/2}}{3\pi^{1/2}(h_0 - h_c)^{3/2}}. \tag{7}$$

In this expression, r_c and h_c represent the critical radium and critical moving distance of upper plate at the beginning of region 3. As we have discussed, τ_y, h_c, and V are constant in Fig. 6(b). It is obvious that σ_C will decrease with the increase of h_0 according to the squeeze flow theory. What is more, the magneto-induced contribution to σ_C will also become smaller due to the attenuation of magnetic field strength with the increase of h_0.

In the absence of magnetic field, particles disperse in the matrix randomly for MR fluids, the chainlike or columnlike microstructures only exist in the presence of an external magnetic field. The compressive force of MR fluids is less than 0.1 N in the absence of magnetic field and can be neglected [Guo *et al.* (2013)]. However, both isotropic and anisotropic particle distributions can be observed for MRP in the absence of magnetic field. The compressive force of MRP without magnetic field is comparable with the one in the presence of magnetic field. Furthermore, compressive property of MRP will be affected by the particle distribution, as can be seen from Fig. 7. All these differences are attributed to the addition of polymer matrix. The polymer matrix can retain the chainlike microstructures after removing the external magnetic field and make a contribution to resist the deformation. Compared with the situation under the magnetic field, it is found that k, n, and σ_C show the increasing trends from isotropic MRP to anisotropic MRP in the absence of magnetic field, to anisotropic MRP in the presence of magnetic field (Table I). Therefore, it can be concluded that the anisotropic microstructures will enhance the the resistance ability of MRP to squeeze, and magnetic field will further improve the strength of particle chains.

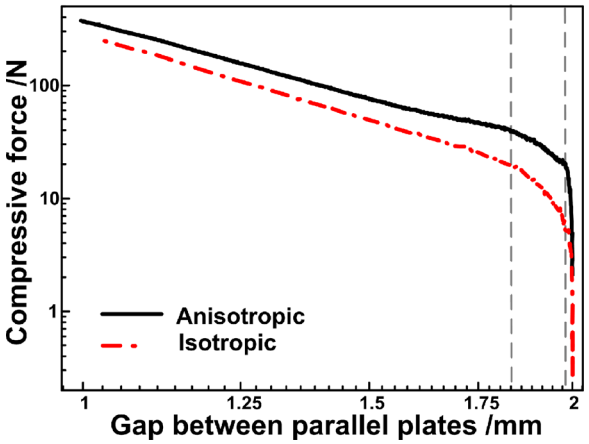

FIG. 7. Compressive forces of MRP-70 with different particle distributions (isotropic and anisotropic) vs gap between parallel plates in the absence of magnetic field in double logarithmic presentation. The initial gap between parallel plates is 2 mm and the compressive velocity is 0.5 mm/min.

Particle concentration is an important influential factor for the squeeze flow behaviors of MRP. As shown in Fig. 8, compressive force of MRP increases with the increase of particle concentration at fixed gap size, which is consistent with the situation in MR fluids [Guo *et al*. (2013); Ruiz-Lopez *et al*. (2012)]. More and thicker particle chains will form for the MRP with high particle concentration under the same magnetic field, which will enhance the magneto-induced strength of MRP and further increase the compressive resistance to deformation. As expected, σ_C increases gradually with the increase of particle concentration. Especially for MRP-80, its σ_C reaches as high as 305.42 kPa under a 445 mT magnetic field, 1.6 times larger than that of MRP-70. The magneto-induced σ_C (the increment of compressive yield stress in the presence of magnetic field to the value in the absence of magnetic field) of MRP-70 under a 291 mT magnetic field is 91.94 kPa, which is 1.84 times larger than that of MR fluids (50 kPa for MR fluids with 30% of volume fraction under a 280 mT magnetic field) reported by Guo *et al*. (2013). It is concluded that the polymer matrix will effectively improve the compressive yield stress of magneto-sensitive materials, which is important in some engineering applications. Finally, it is found that n is also close to the theoretical value ($n = -2.5$) and the influence of particle concentration is clearly reflected from k, which is similar with the situation under different magnetic fields. In other words, the magnetic field and particle concentration have obvious influence on the material properties via k but have nearly no influence on the squeeze flow behavior of MRP (all the parameter n are close to the theoretical value). Ruiz-Lopez *et al*. (2012) proposed a collapse approach for compressive curves of MR fluids to compare with the theoretical prediction. Here, the dimensionless compressive force of MRP with different magnetic fields and particle concentrations as a function of compressive strain is compared. A good collapse of experimental data and well coincidence with the theoretical predication are found (as shown in Fig. S4 from supplementary information).

B. Tensile behaviors of MRP

In tension process, the upper plate moves up to elongate the MRP sample, an opposite loading way in comparison with the compression process. The attractive force of parallel plate decreases with the increase of gap size (i.e., the increase of tensile strain) and increases with the increase of magnetic field [as shown in Fig. 9(a)], which is coincident with the situation in compression process. Figure 9(b) presents the tensile curves of MRP

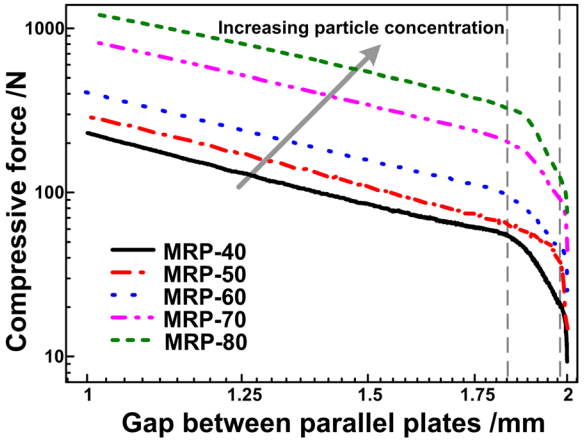

FIG. 8. Compressive forces of MRP with different particle concentrations vs gap between parallel plates in double logarithmic presentation. The initial gap between parallel plates is 2 mm, the compressive velocity is 0.5 mm/min, and the magnetic flux density is 433 mT.

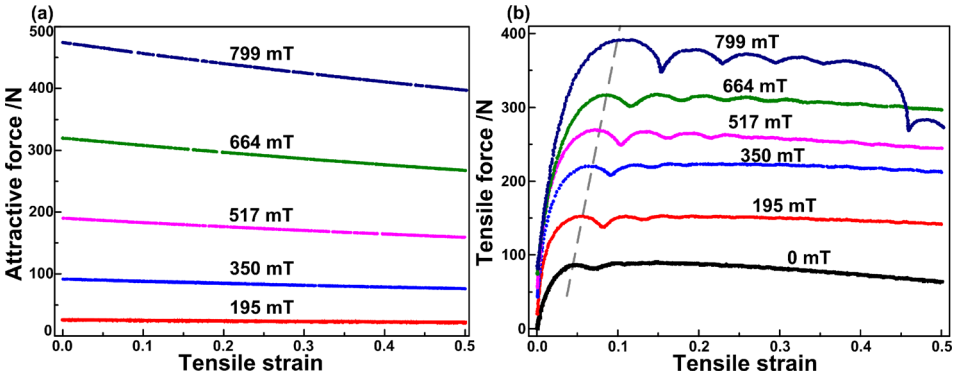

FIG. 9. Attractive forces of parallel plates (a) and tensile forces of MRP-70 (b) under different tensile strains and magnetic fields. The initial gap between parallel plates is 1 mm and the tensile velocity is 0.5 mm/min.

under different magnetic fields. The tensile force increases sharply with the increase of tensile strain at first, then climbs to a peak point. The stress at the position of peak point can be regarded as the tensile yield stress, indicating that the plastic flow begins after the strain exceeds the peak point. In the plastic flow region, the tensile force decreases to a local minimum value and increases to another peak value. Interestingly, the number of peak point is relevant with the magnetic field strength. With the further stretching, the tensile force is almost independent on the strain in the presence of magnetic field. Though different evolution processes of response forces are followed in compression and tension process, three similar deformation regions can observed from both compressive and tensile curves. The tensile behavior of MRP before plastic flow is attributed to the elastic deformation of particle chains and stress relaxation of polymer matrix. In the elastic deformation region, the particle chains are unbroken and the magnetic interaction between particles along the tensile direction gives rise to the sharp increase of tensile force. The relaxation effect of polymer matrix is more and more obvious as time goes on, so it can be found that the increase of tensile force becomes slow with strain before the yield point. After the yield point, the structure failure and reorganization of particle chains, relaxation and slippage of polymer matrix, and attenuation of magnetic field induced by the variation of gap size reach the dynamic balance, thus resulting in an ideal plastic flow for MRP. For a single particle chain, the structure failure and reorganization process is random. Therefore, the tensile force fluctuation is related to statistical integral effect of structure failure and reorganization processes for a large number of particle chains. In this case, the structure failure and reorganization of particle chains happen simultaneously. If the dynamic balance is disrupted, which means the structure failure effect is stronger (or weaker) than the reorganization effect, the tensile force will vary accordingly (i.e., the tensile force fluctuation phenomenon). When a high magnetic field is applied, the particles move more easily due to large magnetic interactions, which make the reorganization of particle chains more easily. However, large magnetic interactions also make the particle chains more fragile. Therefore, more tensile force fluctuations (i.e., the time of structure failure and reorganization of particle chains) can be found for MRP under higher magnetic field at the same tensile distance. In particular, we notice that a collapse of tensile force under a 799 mT magnetic field happens when the tensile strain increases to 0.4, which is a direct evidence that the particle chains under a large magnetic field will become fragile and more easily to fracture due to the quasistatic tensile load.

The tensile stress is mainly affected by the particle chain strength and the interaction strength between the parallel plates and particle chains in MR fluids and ER fluids [Tian *et al.* (2003); Wang *et al.* (2013)]. However, the interaction strength between the parallel

plates and particle chains is not the material property of MR fluids or ER fluids. For MRP, the situation is different. As shown in Figs. 1(b) and 1(c), the MRP sample still adheres to the parallel plate tightly even if fractured from the middle section in the tension process, so it is believed that the tensile force in Fig. 9(b) completely originates from the material itself; the particle chains and the polymer matrix are the main contributors of tensile strength. A linear relationship between tensile yield force and tensile yield strain under different magnetic fields can be found in Fig. 9(b). Magnetic field can change the particle chain strength and further has influence on the tensile behavior of MRP [as shown in Fig. 9(b)]. It can be seen from Fig. 10 that tensile yield stress also linearly increases with the increase of magnetic field. By contrast, the relationship between compressive yield stress and magnetic flux density is plotted in the inset of Fig. 10, and a linear relationship between them can also be found when magnetic flux density is smaller than 667 mT. With the further increase of magnetic field, the compressive yield stress enters saturation region, which means the compressive yield stress almost not change with the variation of magnetic field. Magnetic field dependence of the yield stress for MR fluids has been extensively investigated, but it is still controvesial about this issue [Bossis *et al.* (2002)]. Most people accept that the yield stress and magnetic field meet a power law with an exponent of 1.5 [Chen *et al.* (1998); Phule and Ginder (1999); Rankin *et al.* (1999)], but a linear dependency is also reported by Jiang *et al.* (1998). The mechanisms of yield stress under different deformation processes are different. At shear deformation, the structures are inclined by the shear, and the critical angle at which the rupture occurs scales as $(H/Ms)^{1/2}$, thus giving the $H^{3/2}$ behavior to the shear yield stress (Ms is the saturation magnetization of particle). At the tensile deformation, the particle structures remain almost aligned with the magnetic field. Thus, the tensile yield stress is just the force between particles multiplied by the number of chains per unit surface, so should remain linear with the magnetic field. In addition, the polymer matrix in MRP insulate the adjacent magnetic particles, which will affect the response of particle chains to external stimulus. Therefore, a more complex theoretical model considering the coupling effect between particles and polymer matrix is needed to explain the magnetic field dependence of the yield stress for MRP. The tensile yield stress under a 784 mT magnetic

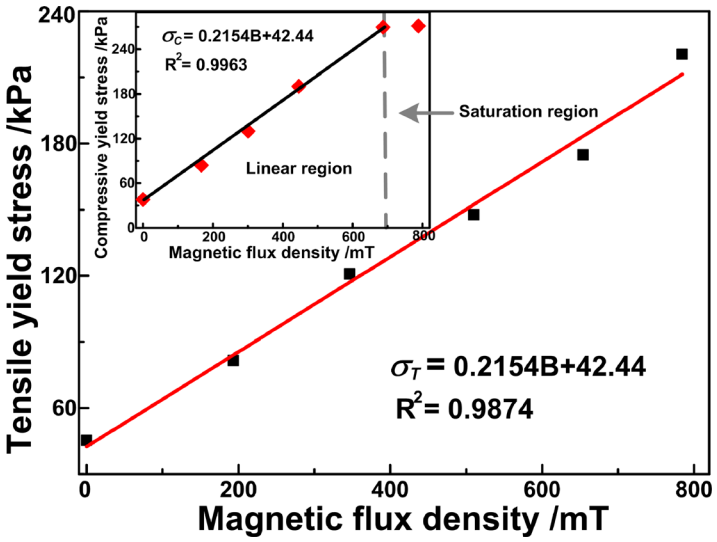

FIG. 10. Tensile yield stress of MRP-70 under different magnetic fields. The inset presents the magnetic field dependency of compressive yield stress.

field (220.43 kPa) is 4.87 times larger than that in the absence of magnetic field (45.27 kPa), suggesting a strong magneto-induced effect on the tensile yield stress. It is also found that the tensile yield stress is smaller than the compressive yield stress under a similar magnetic field condition, which will be further discussed in Sec. III C. For example, the tensile yield stress under a 654 mT magnetic field is 174.80 kPa, while the compressive yield stress under a 683 mT magnetic field is 269.80 kPa. This difference is possibly because the particle chain strength will enhance for the formation of thick chains in the compression process and weaken due to structure failure phenomenon in the tension process.

It is worth mentioning that the tensile stress of MRP in the absence of magnetic field is comparable with the tensile stress in the presence of magnetic field. This part is mainly contributed by the polymer matrix and is affected by the particle distribution. As shown in Fig. 11, the tensile strength of structured MRP is higher than that of MRP with randomly dispersed particles, so is the tensile yield stress. The sharply dropping phenomenon of tensile force after the yield point can also found in anisotropic MRP, which is induced by the fracture of particle chains. With the further increase of tensile strain, the relaxation and slippage of polymer matrix will weaken the tensile strength of MRP. Therefore, a downtrend of tensile force with the increase of gap size after the yield point can be observed in both isotropic and anisotropic MRPs.

As expected, the tensile yield stress of MRP is greatly influenced by the particle concentration (the tensile yield stress of increases from 24.97 kPa for MRP-40 to 187.56 kPa for MRP-80). Moreover, it is found that the tensile behavior is different for MRP with different particle concentrations (Fig. 12). For the MRP with particle weight fraction lower than 60 wt. %, the tensile force continues to increase slowly after the yield point until it begin to collapse at a fixed tensile strain. After the tensile force collapses to a low value, it tends to be stable at this new value. A fluctuation phenomenon of tensile force in the plastic flow region can be observed in MRP-70 and MRP-80. The difference is that a collapse of tensile force appears at the tensile process of MRP-80, and the tensile force of MRP-80 still fluctuates after it drops to a low value. As we have discussed, the structure failure and reorganization of particle chains are the essential reasons for the tensile force fluctuation. If the particle concentration is low, the reorganization of particle chains will not happen because there are not enough number of particles to form intact chains when

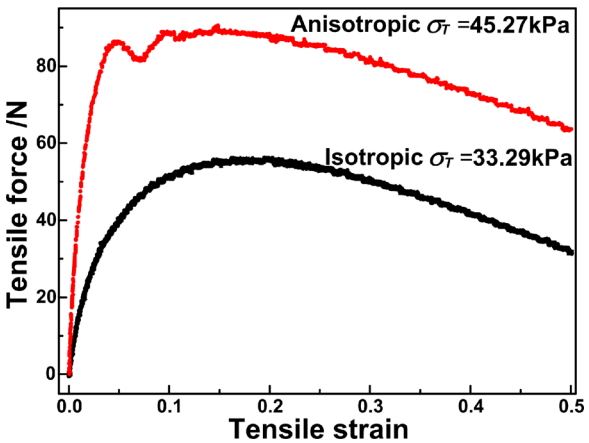

FIG. 11. Tensile forces of MRP-70 with different particle distributions (isotropic and anisotropic) under different tensile strains in the absence of magnetic field. The initial gap between parallel plates is 1 mm and the tensile velocity is 0.5 mm/min.

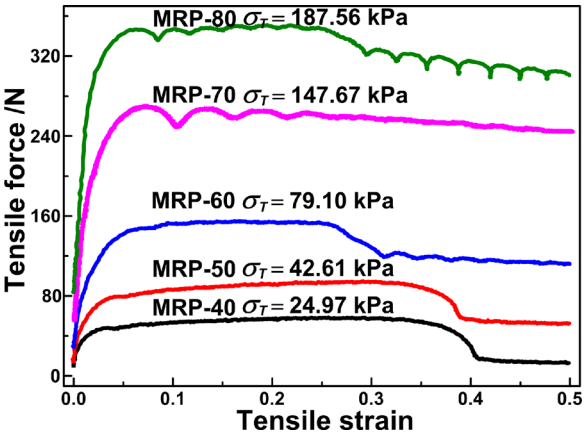

FIG. 12. Tensile forces of MRP with different particle concentrations under different tensile strains. The initial gap between parallel plates is 1 mm, the tensile velocity is 0.5 mm/min, and the magnetic flux density is 517 mT.

the gap size becomes more and more large, so the fluctuation phenomenon will not happen in the MRP with low particle concentration. Except for magnetic field, high particle concentration will also make MRP more fragile and more easily to be fractured by a tensile load. Therefore, the collapse of tensile force for the MRP with high particle concentration is dominated by the fracture of particle chains, different from the situation in the MRP with low particle concentration (the collapse of tensile force of MRP with low particle concentration is mainly determined by the tensile property of polymer matrix). If the particle concentration is moderate, the collapse mechanisms of tensile force from particle and matrix will restrict each other, thus enhancing the tension toughness of MRP and no collapse phenomenon can be observed in the strain range of 0–0.5 (such as MRP-70 in Fig. 12).

C. Oscillatory squeeze behaviors of MRP

The compressive and tensile behaviors of MRP that we have discussed above reflect the quasistatic mechanical performance. The dynamic mechanical behavior is another important aspect to assess the performance of MRP for academia as well as for some potential applications [Farjoud *et al.* (2009); Farjoud *et al.* (2011); Kulkarni *et al.* (2003)]. Oscillatory shear mode is the mostly used dynamic characterization method to investigate the rheological properties of MR fluids [de Vicente *et al.* (2011b)], while the oscillatory squeeze behaviors of MR fluids are paid less attention though it is also valuable to understand the MR mechanism. Next, the oscillatory squeeze behaviors of MRP under constant volume will be experimentally studied. In the meantime, the influences of oscillatory amplitude, magnetic field, particle distribution, and particle concentration on the oscillatory squeeze properties of MRP will also be discussed.

For the oscillatory squeeze tests, the tension process is defined when the displacement is positive while the negative displacement represents the sample is under compression. Hysteresis loop appears when no MRP is placed between parallel plates in the presence of magnetic field [Fig. 13(a)], indicating energy dissipation companies the relative movement of parallel plates. In comparison with the hysteresis loops of MRP [Fig. 13(b)], the dissipated energy generated by the relative movement of parallel plates can be neglected, which can also be compared more obviously in Fig. 14(a). The attractive force between parallel plates decreases with the increase of gap size, consistent with the quasistatic

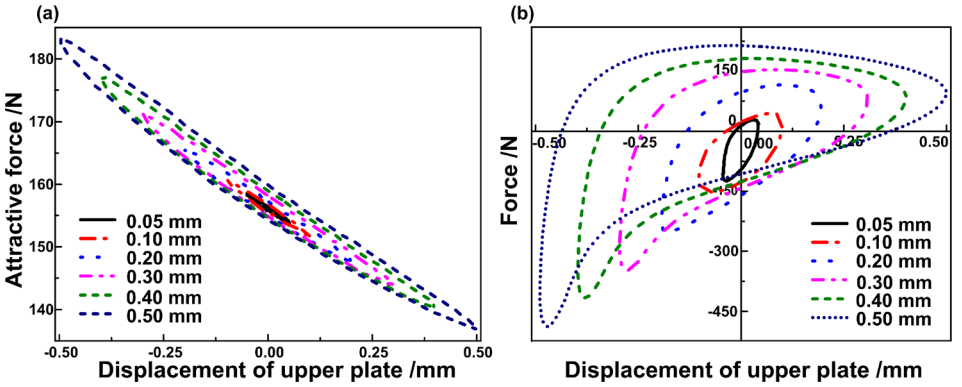

FIG. 13. Force-displacement curves (hysteresis loops) of parallel plates (a) and MRP-70 (b) at different oscillatory amplitudes. The initial gap between parallel plates is 2 mm, the oscillatory frequency is 1 Hz, and the magnetic flux density is 433 mT.

situation. In addition, the shape of hysteresis loops in Fig. 13(a) is almost symmetric while asymmetric force-displacement curves are found in Fig. 13(b). The hysteresis loop of MRP under oscillatory shear mode is also symmetric [Gong *et al.* (2012)]; the asymmetry of hysteresis loop under oscillatory squeeze mode reflects the difference of compressive and tensile behaviors of MRP. For further investigating the oscillatory squeeze behaviors of MRP, we compared the maximum tensile force $F_{T\text{-}max}$ and the maximum compressive force $F_{C\text{-}max}$ in different hysteresis loops. Dissipated energy density E_d can be obtained by calculating the area of the hysteresis loop per unit volume, which can be used for a characterization parameter of damping performance. Moreover, equivalent viscous damping coefficient c_e is also a characterization parameter related to material damping, which is defined as

$$c_e = \frac{W_c}{\pi \omega A^2}, \tag{8}$$

where W_c is the dissipated energy in an oscillatory cycle. ω and A present the angular frequency and oscillatory amplitude, respectively. These main parameters (as shown in Table II) obtained from experimental results can be used to characterize the oscillatory squeeze behaviors of MRP.

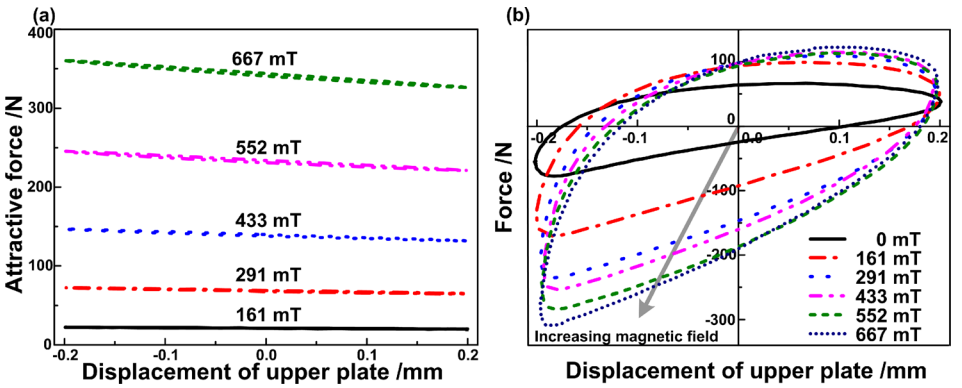

FIG. 14. Force-displacement curves (hysteresis loops) of attraction between parallel plates (a) and MRP-70 (b) under different magnetic fields. The initial gap between parallel plates is 2 mm, the oscillatory frequency is 1 Hz, and the oscillatory amplitude is 0.2 mm.

From Table II, we can see that all of $F_{T\text{-}max}$, $F_{C\text{-}max}$, and E_d increase sharply with the increase of oscillatory amplitude, but c_e shows an opposite tendency. At the same oscillatory frequency, large oscillatory amplitude means high loading rate. The strain-rate effect will enhance the resistance of MRP to deformation. In compression process, both the contact area between MRP and plates and magnetic field strength will increase with the decreasing of gap size; these will also enhance the resistance of MRP to compressive deformation while they will play a weakening role on resistance of MRP to deformation on the tensile side. This analysis qualitatively explains the reason of oscillatory amplitude dependence of $F_{T\text{-}max}$ and $F_{C\text{-}max}$ and the asymmetry of force-displacement curves. Dissipated energy W_c is directly relevant with the force and displacement in the oscillatory cycle, so it is easy to understand the oscillatory amplitude dependence of E_d. According to the definition of Eq. (8), the denominator is proportional to the square of the oscillatory amplitude at fixed oscillatory frequency, which means the denominator increases faster than the numerator with the increase of oscillatory amplitude. In consequence, a decreasing c_e with the increasing oscillatory amplitude is given in Table II.

External magnetic field will change the magnetic interaction between particles and further control the oscillatory squeeze behaviors of MRP [as shown in Fig. 14(b)]. Therefore, it can be found in Table II that all the related parameters vary as the magnetic field changes. The magneto-induced effect is more obvious under low magnetic field than under high magnetic field. High magneto-sensitivity of MRP under low magnetic field is valuable in practical applications because high magnetic field is difficult to be achieved. In addition, it is worth mentioning that the dissipated energy W_c of MRP in an oscillatory cycle and c_e will increase with the increase of magnetic field (Table II). The increasement of W_c is attributed to the increasing damping force under high magnetic field while the variation of c_e also originates from the magneto-induced damping force.

In comparison with the quasistatic situation (Figs. 7 and 11), the particle distribution has nearly no influence on the oscillatory squeeze behavior of MRP (the hysteresis loops of MRP with different particle distributions are almost coincident, as shown in Fig. 15). In the absence of magnetic field, the particle chains in the anisotropic MRP will be completely destroyed after dozens of oscillatory cycles (the sixtieth force-displacement curve

TABLE II. The related experimental parameters of MRP under different oscillatory squeeze tests.

Particle distribution	W (wt. %)	B (mT)	A (mm)	$F_{T\text{-}max}$ (N)	$F_{C\text{-}max}$ (N)	E_d (kJ m^{-3})	c_e ($\times 10^5$) (kg s^{-1})
Isotropic	70	0	0.2	66.74	77.39	15.25	0.38
Anisotropic	70	0	0.2	70.67	79.10	16.01	0.40
Anisotropic	70	161	0.2	99.07	170.55	31.31	0.78
Anisotropic	70	291	0.2	109.11	234.65	39.97	0.99
Anisotropic	70	433	0.2	113.05	254.26	41.47	1.03
Anisotropic	70	552	0.2	115.49	283.27	45.29	1.12
Anisotropic	70	667	0.2	122.57	309.69	45.59	1.14
Anisotropic	70	433	0.05	28.58	124.25	3.89	1.55
Anisotropic	70	433	0.1	45.17	152.78	12.71	1.26
Anisotropic	70	433	0.3	153.37	348.10	76.63	0.85
Anisotropic	70	433	0.4	181.72	415.22	110.39	0.69
Anisotropic	70	433	0.5	213.49	486.78	146.27	0.58
Anisotropic	40	433	0.3	55.27	75.93	15.81	0.17
Anisotropic	50	433	0.3	112.42	166.19	49.67	0.55
Anisotropic	60	433	0.3	142.46	296.87	60.86	0.67
Anisotropic	80	433	0.3	184.91	424.89	100.69	1.11

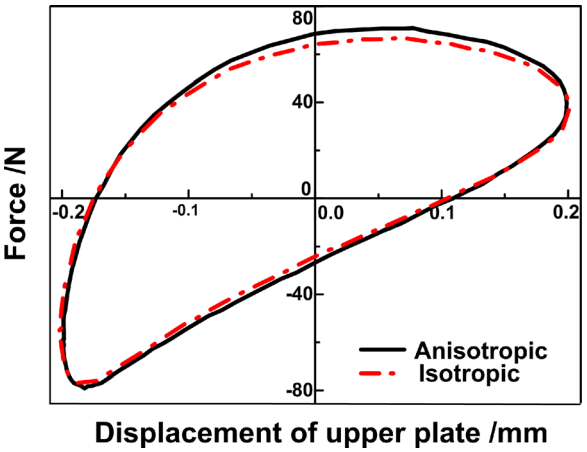

FIG. 15. Force-displacement curves (hysteresis loops) of MRP-70 with different particle distributions (isotropic and anisotropic) in the absence of magnetic field. The initial gap between parallel plates is 2 mm, the oscillatory frequency is 1 Hz, and the oscillatory amplitude is 0.2 mm.

is chosen in all the oscillatory squeeze tests) because no magnetic interaction drives particles to reorganize chainlike microstructures during the oscillatory squeeze process. Finally, the particles in the anisotropic MRP tend to disperse uniformly as those in the isotropic MRP, resulting in a similar oscillatory squeeze behavior. It is deduced from this result that the structure effect is not important under oscillatory squeeze mode even in the presence of magnetic field because the oscillatory squeeze process is so fast that the particles have no enough time to form chainlike structures.

Figure 16 shows the hysteresis loops of MRP with different particle concentrations under a 433 mT magnetic field. As expected, the oscillatory squeeze behaviors of MRP are highly dependent on the particle concentration. The magneto-induced strength of MRP will be enhanced by large magnetic interaction between particles in the MRP with high particle concentration under the same magnetic field, which means $F_{T\text{-}max}$ and $F_{C\text{-}max}$ will increase accordingly. Meanwhile, the friction between particles and polymer

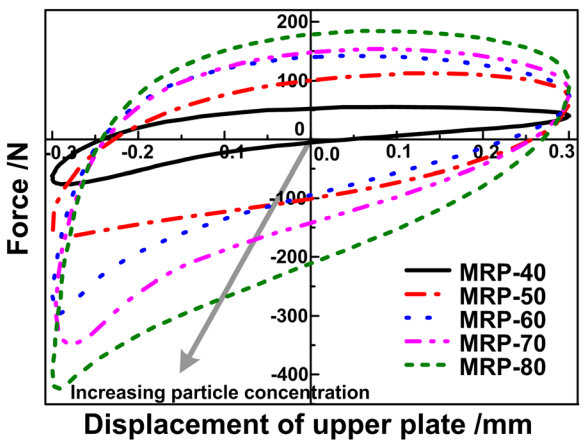

FIG. 16. Force-displacement curves (hysteresis loops) of MRP with different particle concentrations. The initial gap between parallel plates is 2 mm, the oscillatory frequency is 1 Hz, the oscillatory amplitude is 0.3 mm, and the magnetic flux density is 433 mT.

matrix will greatly increase with the increase of particle concentration, resulting in the increase of E_d. The increasing c_e indicates the damping performance of MRP is sensitive to the particle concentration. It can be concluded that the anisotropic microstructures will enhance the resistance ability of MRP to squeeze, and magnetic field will further improve the strength of particle chains.

IV. CONCLUSIONS

In this work, the compressive, tensile, and oscillatory squeeze behaviors of MRP were systematically studied for the first time. Due to the existence of polymer matrix, the squeeze flow behaviors of MRP are more complicated than those of MR fluids. Three flow regions (elastic deformation region, stress relaxation region, and plastic flow region) can be found in both quasistatic compression and tension processes. The stress relaxation region mainly originates from the polymer matrix. In addition, the polymer matrix can enhance the yield stress under compression and tension processes as well (the yield stress of MRP is higher than that of MR fluids under similar experimental condition). Even no magnetic field is applied, the yield stress of MRP is also comparable with that in the presence of magnetic field, which is still contributed from the polymer matrix.

As a magneto-sensitive smart material, high magneto-induced effect of MRP is found from compressive and tensile behaviors. For example, the compressive yield stress under a 764 mT magnetic field (271.43 kPa) can be 7.13 times larger than that in the absence of magnetic field (38.08 kPa), while the tensile yield stress under a 764 mT magnetic field (207.01 kPa) can be 4.57 times larger than that in the absence of magnetic field (45.27 kPa). The initial particle distribution has great influence on the compressive and tensile behaviors of MRP, but the difference of hysteresis loops between isotropic and anisotropic MRP under oscillatory squeeze mode is negligible. From hysteresis loops under oscillatory squeeze mode, the damping performance of MRP can be assessed. The dissipated energy density and equivalent viscous damping coefficient are sensitive to the oscillatory amplitude, magnetic field, and particle concentration, which are valuable for the designing of damping devices. Moreover, the different characteristics of MRP under compressive and tensile processes result in the asymmetry of hysteresis loop under oscillatory squeeze mode.

ACKNOWLEDGMENTS

Financial supports from the National Natural Science Foundation of China (Grant Nos. 11125210, 11072234, 11102202) and the National Basic Research Program of China (973 Program, Grant No. 2012CB937500) are gratefully acknowledged.

References

Ahn, Y. K., J. Y. Ha, and B. S. Yang, "A new type controllable squeeze film damper using an electromagnet," J. Vib. Acoust. **126**, 380–383 (2004).

An, H. N., B. Sun, S. J. Picken, and E. Mendes, "Long time response of soft magnetorheological gels," J. Phys. Chem. B **116**, 4702–4711 (2012).

An, H. N., S. J. Picken, and E. Mendes, "Enhanced hardening of soft self-assembled copolymer gels under homogeneous magnetic fields," Soft Matter **6**, 4497–4503 (2010).

Bossis, G., O. Volkova, S. Lacis, and A. Meunier, "Magnetorheology: Fluids, structures and rheology," Ferrofluids Lect. Notes Phys. **594**, 202–230 (2002).

Carmignani, C., P. Forte, and E. Rustighi, "Design of a novel magneto-rheological squeeze-film damper," Smart Mater. Struct. **15**, 164–170 (2006).

Chen, L., X. L. Gong, W. Q. Jiang, J. J. Yao, H. X. Deng, and W. H. Li, "Investigation on magnetorheological elastomers based on natural rubber," J. Mater. Sci. **42**, 5483–5489 (2007).

Chen Z. Y., X. Tang, G. C. Zhang, Y. Jin, W. Ni, and Y. R. Zhu, "A novel approach of preparing ultrafine magnetic metallic particles and the magnetorheology measurements for suspensions containing these particles," in *Proceedings of the 6th International Conference on ER Fluids, MR Suspensions and Their Applications*, Yonezawa, 22–25 July, 1997, edited by M. Nakano and K. Koyama (World Scientific, Singapore, 1998), pp. 486–493.

Choi, S. B., H. J. Choi, Y. T. Choi, and N. M. Wereley, "Preparation and mechanical characteristics of poly (methylaniline) based electrorheological fluid," J. Appl. Polym. Sci. **96**, 1924–1929 (2005).

Chu, S. H., S. J. Lee, and K. H. Ahn, "An experimental study on the squeezing flow of electrorheological suspensions," J. Rheol. **44**, 105–120 (2000).

de Vicente, J., D. J. Klingenberg, and R. Hidalgo-Alvarez, "Magnetorheological fluids: A review," Soft Matter **7**, 3701–3710 (2011b).

de Vicente, J., J. Antonio Ruiz-Lopez, E. Andablo-Reyes, J. Pablo Segovia-Gutierrez, and R. Hidalgo-Alvarez, "Squeeze flow magnetorheology," J. Rheol. **55**, 753–779 (2011a).

Farjoud, A., M. Craft, W. Burke, and M. Ahmadian, "Experimental investigation of MR squeeze mounts," J. Intell. Mater. Syst. Struct. **22**, 1645–1652 (2011).

Farjoud, A., R. Cavey, M. Ahmadian, and M. Craft, "Magneto-rheological fluid behavior in squeeze mode," Smart Mater. Struct. **18**, 095001 (2009).

Fuhrer, R., E. K. Athanassiou, N. A. Luechinger, and W. J. Stark, "Crosslinking metal nanoparticles into the polymer backbone of hydrogels enables preparation of soft, magnetic field-driven actuators with muscle-like flexibility," Small **5**, 383–388 (2009).

Gomez-Ramirez, A., P. Kuzhir, M. T. Lopez-Lopez, G. Bossis, A. Meunier, and J. D. G. Duran, "Steady shear flow of magnetic fiber suspensions: Theory and comparison with experiments," J. Rheol. **55**, 43–67 (2011).

Gong, X. L., Y. G. Xu, S. H. Xuan, C. Y. Guo, L. H. Zong, and W. Q. Jiang, "The investigation on the nonlinearity of plasticine-like magnetorheological material under oscillatory shear rheometry," J. Rheol. **56**, 1375–1391 (2012).

Guo, C. Y., X. L. Gong, S. H. Xuan, Q. F. Yan, and X. H. Ruan, "Squeeze behavior of magnetorheological fluids under constant volume and uniform magnetic field," Smart Mater. Struct. **22**, 045020 (2013).

Jiang, F. Q., Z. W. Wang, J. Y. Wu, L. W. Zhou, and Z. Y. Ying, "Magnetorheological materials and their application in shock absorbers," in *Proceedings of the 6th International Conference on ER Fluids, MR Suspensions and Their Applications*, Yonezawa, 22–25 July, 1997, edited by M. Nakano and K. Koyama (World Scientific, Singapore, 1998), pp. 494–501.

Kulkarni, P., C. Ciocanel, S. L. Vieira, and N. Naganathan, "Study of the behavior of MR fluids in squeeze, torsional and valve modes," J. Intell. Mater. Syst. Struct. **14**, 99–104 (2003).

Li, W. H., Y. Zhou, and T. F. Tian, "Viscoelastic properties of MR elastomers under harmonic loading," Rheol. Acta **49**, 733–740 (2010).

Liu, T. X., Y. G. Xu, X. L. Gong, H. M. Pang, and S. H. Xuan, "Magneto-induced normal stress of magnetorheological plastomer," AIP Adv. **3**, 082122 (2013a).

Liu, X. H., Q. Q. Chen, and H. Lu, "Research on the mechanical property of magnetorheological fluids microstructure under compression working mode," Optoelectron. Adv. Mater., Rapid Commun. **7**, 231–239 (2013b).

Mazlan, S. A., A. Issal, and A. G. Olabi, "Magnetorheological fluids behaviour in tension loading mode," Adv. Mater. Res. **47–50**(Pts. 1 and 2), 242–245 (2008b).

Mazlan, S. A., I. Ismail, H. Zamzuri, and A. Y. Abd Fatah, "Compressive and tensile stresses of magnetorheological fluids in squeeze mode," Int. J. Appl. Electromagn. Mech. **36**, 327–337 (2011).

Mazlan, S. A., N. B. Ekreem, and A. G. Olabi, "The performance of magnetorheological fluid in squeeze mode," Smart Mater. Struct. **16**, 1678–1682 (2007).

Mazlan, S. A., N. B. Ekreem, and A. G. Olabi, "An investigation of the behaviour of magnetorheological fluids in compression mode," J. Mater. Process. Technol. **201**, 780–785 (2008a).

McIntyre, E. C., and F. E. Filisko, "Squeeze flow of electrorheological fluids under constant volume," J. Intell. Mater. Syst. Struct. **18**, 1217–1220 (2007).

McIntyre, E. C., and F. E. Filisko, "Filtration in electrorheological suspensions related to the Peclet number," J. Rheol. **54**, 591–603 (2010).

Mitsumata, T., A. Honda, H. Kanazawa, and M. Kawai, "Magnetically tunable elasticity for magnetic hydrogels consisting of carrageenan and carbonyl iron particles," J. Phys. Chem. B **116**, 12341–12348 (2012).

Mitsumata, T., and N. Abe, "Magnetic-field sensitive gels with wide modulation of dynamic modulus," Chem. Lett. **38**, 922–923 (2009).

Mitsumata, T., and S. Ohori, "Magnetic polyurethane elastomers with wide range modulation of elasticity," Polym. Chem. **2**, 1063–1067 (2011).

Nguyen, V. Q., A. S. Ahmed, and R. V. Ramanujan, "Morphing soft magnetic composites," Adv. Mater. **24**, 4041–4054 (2012).

Olabi, A. G., and A. Grunwald, "Design and application of magneto-rheological fluid," Mater. Des. **28**, 2658–2664 (2007).

Park, B. J., F. F. Fang, and H. J. Choi, "Magnetorheology: Materials and application," Soft Matter **6**, 5246–5253 (2010).

Phule, P. P., and J. M. Ginder, "Synthesis and properties of novel magnetorheological fluids having improved stability and redispersibility," Int. J. Mod. Phys. B **13**, 2019–2027 (1999).

Rankin, P. J., A. T. Horvath, and D. J. Klingenberg, "Magnetorheology in viscoplastic media," Rheol. Acta **38**, 471–477 (1999).

Ruiz-Lopez, J. A., R. Hidalgo-Alvarez, and J. de Vicente, "On the validity of continuous media theory for plastic materials in magnetorheological fluids under slow compression," Rheol. Acta **51**, 595–602 (2012).

See, H., J. S. Field, and B. Pfister, "The response of electrorheological fluid under oscillatory squeeze flow," J. Non-Newtonian Fluid Mech. **84**, 149–158 (1999).

Tang, X., X. Zhang, R. Tao, and Y. M. Rong, "Structure-enhanced yield stress of magnetorheological fluids," J. Appl. Phys. **87**, 2634–2638 (2000).

Tian, Y., and Q. Zou, "Normalized method for comparing tensile behaviors of electrorheological fluids," Appl. Phys. Lett. **82**, 4836–4838 (2003).

Tian, Y., Q. Zou, Y. G. Meng, and S. Z. Wen, "Tensile behavior of electrorheological fluids under direct current electric fields," J. Appl. Phys. **94**, 6939–6944 (2003).

Wang, H. Y., C. Bi, J. W. Kan, C. F. Gao, and W. Xiao, "The Mechanical property of magnetorheological fluid under compression, elongation, and shearing," J. Intell. Mater. Syst. Struct. **22**, 811–816 (2011).

Wang, H. Y., C. Bi, Z. H. Zhang, J. W. Kan, and C. F. Gao, "An investigation of tensile behavior of magnetorheological fluids under different magnetic fields," J. Intell. Mater. Syst. Struct. **24**, 541–547 (2013).

Wang, J., G. Meng, N. Feng, and E. J. Hahn, "Dynamic performance and control of squeeze mode MR fluid damper-rotor system." Smart Mater. Struct. **14**, 529–539 (2005).

Wilson, M. J., A. Fuchs, and F. Gordaninejad, "Development and characterization of magnetorheological polymer gels," J. Appl. Polym. Sci. **84**, 2733–2742 (2002).

Xu, Y. G., X. L. Gong, and S. H. Xuan, "Soft magnetorheological polymer gels with controllable rheological properties," Smart Mater. Struct. **22**, 075029 (2013).

Xu, Y. G., X. L. Gong, S. H. Xuan, W. Zhang, and Y. C. Fan, "A high-performance magnetorheological material: Preparation, characterization and magnetic-mechanic coupling properties," Soft Matter **7**, 5246–5254 (2011).

Xu, Y. G., X. L. Gong, S. H. Xuan, X. F. Li, L. J. Qin, and W. Q. Jiang, "Creep and recovery behaviors of magnetorheological plastomer and its magnetic-dependent properties," Soft Matter **8**, 8483–8492 (2012).

Yang, F. Q., "Tension and compression of electrorheological fluid," J. Colloid Interface Sci. **192**, 162–165 (1997).

Zhang, X. Z., X. L. Gong, P. Q. Zhang, and Q. M. Wang, "Study on the mechanism of the squeeze-strengthen effect in magnetorheological fluids," J. Appl. Phys. **96**, 2359–2364 (2004).

See supplementary material at http://dx.doi.org/10.1122/1.4869350 for the experimental approach to obtain the compressive (or tensile) force of MRP and the dimensionless compressive force of MRP with different particle concentrations and different magnetic fields.